



KARRIKIN UP-REGULATED F-BOX 1 (KUF1) imposes negative feedback regulation of karrikin and KAI2 ligand metabolism in *Arabidopsis thaliana*

Claudia Sepulveda^a, Michael A. Guzmán^a, Qingtian Li^a, José Antonio Villaécija-Aguilar^b, Stephanie E. Martinez^a, Muhammad Kamran^c, Aashima Khosla^a, Wei Liu^d, Joshua M. Gendron^d, Caroline Gutjahr^b, Mark T. Waters^c, and David C. Nelson^{a,1}

Edited by Uta Paszkowski, University of Cambridge, Cambridge, United Kingdom; received July 13, 2021; accepted January 28, 2022 by Editorial Board Member Julian I. Schroeder

Karrikin (KAR) molecules found in smoke stimulate seed germination of many plant species that emerge after fire. Genetic studies in *Arabidopsis thaliana* have identified core components of the KAR signaling pathway, including an α/β -hydrolase, KARRIKIN INSENSITIVE2 (KAI2), that is required for KAR responses. Although KAI2 is often considered a KAR receptor, recent evidence suggests that KARs may require metabolism to become bioactive signals. In addition to sensing KARs or a KAR-derived signal, KAI2 is thought to recognize an unknown endogenous signal, KAI2 ligand (KL). We generated loss-of-function mutations in *KARRIKIN-UP-REGULATED F-BOX1* (*KUF1*), which is a transcriptional marker of KAR/KL signaling in *A. thaliana* and other plants. The *kuf1* mutant in *Arabidopsis* shows several phenotypes that are consistent with enhanced activity of the KAI2 pathway, including reduced hypocotyl elongation, enhanced cotyledon expansion in light-grown seedlings, increased root hair density and elongation, and differential expression of KAR/KL-responsive transcriptional markers. Seedling phenotypes of *kuf1* are dependent on KAI2 and its signaling partner MORE AXILLARY GROWTH2 (MAX2). Furthermore, *kuf1* mutants are hypersensitive to KAR₁, but not to other molecules that can signal through KAI2 such as GR24. This implies that *kuf1* does not increase the overall responsiveness of the KAI2-dependent signaling pathway, but specifically affects the ability of KAI2 to detect certain signals. We hypothesize that KUF1 imposes feedback inhibition of KL biosynthesis and KAR₁ metabolism. As an F-box protein, KUF1 likely participates in an E3 ubiquitin ligase complex that imposes this regulation through polyubiquitylation of a protein target(s).

plant hormones | signaling | proteolysis | biosynthesis | photomorphogenesis

Plants have evolved several adaptations that enable rapid regrowth in the postfire environment, including germination of buried seeds in response to chemical cues in smoke. Approximately 1,200 angiosperms are known to have positive germination responses to smoke or smoke-water treatments (1). A potent germination stimulant, 3-methyl-2H-furo[2,3-*c*]pyran-2-one (KAR₁), was identified in smoke in 2004, followed by several similar butenolide compounds now known as karrikins (KARs) (2, 3). Unexpectedly, KAR responses are neither limited to germination nor to species from fire-prone environments. For example, KARs enhance *Arabidopsis thaliana* germination and seedling growth responses to light (4, 5). Smoke-water and/or KAR₁ treatment have also been reported to enhance seedling vigor or accelerate development of several crop plants (6, 7). The capacity to respond to KARs may be widespread among angiosperms, with some fire-following species having evolved more sensitive germination responses to KARs (1, 8).

Two genes are required for KAR responses in *A. thaliana*. The first is *MORE AXILLARY GROWTH2* (*MAX2*), which encodes an F-box protein that is also necessary for responses to the plant hormone strigolactone (SL) (9–11). As an F-box protein, MAX2 functions as a substrate-specifying component of SCF (Skp1, Cullin1, F-box) E3 ubiquitin ligase complexes, which mark proteins for degradation by attaching polyubiquitin chains. The second is *KARRIKIN INSENSITIVE2* (*KAI2*)/*HYPOSENSITIVE TO LIGHT* (*HTL*), an ancient paralog of the SL receptor *DWARF14* (*D14*)/*DECREASED APICAL DOMINANCE2* (*DAD2*). *KAI2* and *D14* encode α/β -hydrolases with strictly conserved Ser-His-Asp catalytic triads that are important for their signaling activity (12). During SL signaling, a methylbutenolide “D-ring” moiety of SL is hydrolyzed by D14 and covalently attached to the catalytic His residue (13, 14). It is currently under debate which step in the process of SL binding, hydrolysis, and release constitutes

Significance

Karrikins are chemicals in smoke that stimulate regrowth of many plants after fire. However, karrikin responses are not limited to species from fire-prone environments and can affect growth after germination. Putatively, this is because karrikins mimic an unknown signal in plants, KAI2 ligand (KL). Karrikins likely require modification in plants to become bioactive. We identify a gene, *KUF1*, that appears to negatively regulate biosynthesis of KL and metabolism of a specific karrikin. *KUF1* expression increases in response to karrikin or KL signaling, thus forming a negative feedback loop that limits further activation of the signaling pathway. This discovery will advance understanding of how karrikins are perceived and how smoke-activated germination evolved. It will also aid identification of the elusive KL.

Author contributions: C.S., M.A.G., Q.L., J.A.V.-A., J.M.G., C.G., M.T.W., and D.C.N. designed research; C.S., M.A.G., Q.L., J.A.V.-A., S.E.M., M.K., and W.L. performed research; C.S., M.A.G., Q.L., and A.K. contributed new reagents/analytic tools; C.S., M.A.G., Q.L., J.A.V.-A., S.E.M., M.K., C.G., M.T.W., and D.C.N. analyzed data; and C.G., M.T.W., and D.C.N. wrote the paper.

The authors declare no competing interest.

This article is a PNAS Direct Submission. U.P. is a guest editor invited by the Editorial Board.

Copyright © 2022 the Author(s). Published by PNAS. This article is distributed under Creative Commons Attribution-NonCommercial-NoDerivatives License 4.0 (CC BY-NC-ND).

¹To whom correspondence may be addressed. Email: david.nelson@ucr.edu.

This article contains supporting information online at <http://www.pnas.org/lookup/suppl/doi:10.1073/pnas.2112820119/-DCSupplemental>.

Published March 7, 2022.

activation of D14 (13–15). Regardless, SL induces a conformational change in D14 that promotes its association with SCF^{MAX2} and a subclade of proteins in the SMAX1-LIKE (SMXL) family that are orthologous to the rice protein DWARF53 (D53). D53-type SMXL proteins (i.e., SMXL6, SMXL7, and SMXL8 in *Arabidopsis*) are then polyubiquitinated and rapidly degraded by the 26S proteasome, activating the expression of downstream genes that carry out growth responses to SLs (13, 16–18). KAR signaling proceeds similarly. Activation of KAI2 promotes interactions with SCF^{MAX2} and the target proteins SMAX1 and SMXL2, leading to their polyubiquitination and proteolysis (19–23). In addition to mediating KAR signaling, *Arabidopsis* KAI2 responds to GR24^{ent-5DS}, a component of racemic GR24 (*rac*-GR24) whose D-ring is in a 2′S stereochemical configuration that is not found in natural SLs. Although *rac*-GR24 is commonly used as a synthetic SL analog, its constituent enantiomers GR24^{5DS} and GR24^{ent-5DS} preferentially activate D14 and KAI2, respectively (24, 25).

KARs have been detected in smoke-water, postfire soil, and biochars, but there is currently no evidence that KARs are produced by living plants (3, 26, 27). Thus KARs may be strictly abiotic, or at least nonplant, signals. However, growing evidence suggests that KARs mimic an endogenous signal in plants that is recognized by KAI2 (28–30). For example, *kai2* and *max2* have several phenotypes that are not found in *d14* or SL biosynthesis mutants (9) and are opposite to the effects of applied KAR. Although the putative KAI2 ligand (KL) remains unknown, insights into its functions can be gained by examining *kai2* phenotypes and by using KARs or chemicals such as GR24^{ent-5DS} or desmethyl-GR24 (dGR24) as substitutes (24, 31). Mutant *kai2* seeds have increased dormancy, while *kai2* seedlings have impaired photomorphogenesis that results in elongated hypocotyls and reduced cotyledon expansion (12). Recent studies have expanded the known roles of KAI2, and by proxy KAR/KL signaling, beyond germination and seedling growth. In rice, KAI2 is necessary for the formation of symbiotic interactions with arbuscular mycorrhizal fungi (32, 33). In *Arabidopsis*, KAI2 influences the shape of leaves, promotes several drought and abiotic stress resistance traits, increases root hair density, and promotes root hair elongation (34–37). In the liverwort *Marchantia polymorpha*, a KAI2-SCF^{MAX2}-SMAX1 signaling pathway regulates thallus growth and orientation and cell proliferation in gemmae (38).

Because KAI2 is necessary for KAR responses and has been demonstrated to bind KAR₁, it is often referred to in the literature as a KAR receptor. This may be misleading, however, as there is conflicting evidence that KARs can activate KAI2 directly. Several studies have demonstrated KAR₁ binding by KAI2 through isothermal calorimetry, equilibrium microdialysis, intrinsic fluorescence, heteronuclear single quantum coherence, and dye-based thermal denaturation assays (39–45). These methods produced *K_d* estimates for KAR₁ ranging from 5 μM to 147 μM for *Arabidopsis* KAI2, which indicates a lower affinity than expected considering KAR₁ affects *Arabidopsis* growth at 1 μM and lower concentrations.

It must be considered that evidence of a molecule binding to a receptor is not necessarily evidence that the receptor is activated. Differential scanning fluorimetry (DSF) has emerged as a useful tool to identify ligands that activate D14. Upon exposure to a SL, D14 undergoes a shift in melting temperature that presumably reflects a conformational change or propensity for structural shifts (46). The abilities of different SL analogs to trigger a melting temperature shift in D14 correlates well with their bioactivities, although the extent of the temperature shift

can vary in different D14 proteins (13, 15, 47, 48). Similarly, KAI2 undergoes destabilization in DSF assays in the presence of *rac*-GR24 and GR24^{ent-5DS}, consistent with KAI2-mediated growth responses to these chemicals, and an intact catalytic triad is required to do so. However, KAI2 shows no response to KAR₁ or KAR₂ in DSF assays (8, 29). Similarly, yeast two-hybrid (Y2H) interactions between KAI2 and SMAX1 are promoted by *rac*-GR24 and GR24^{ent-5DS}, but not by KAR₁ or KAR₂ (22). Therefore, in yeast and in DSF assays, KARs are not equivalent agonists to GR24.

Recent evidence suggests that this is also true in plants. Coimmunoprecipitation (Co-IP) of SMAX1 and SMXL2 by KAI2 is triggered by GR24^{ent-5DS}, but KAR₁ and 2′R-configured GR24 stereoisomers (e.g., GR24^{5DS}) are ineffective at stimulating KAI2-SMXL2 interactions. KAR₁ is also much slower than GR24^{ent-5DS} to induce polyubiquitination and degradation of SMXL2 (23). This raises the possibility that KAR₁ requires metabolism in plants to become an active ligand for KAI2, but GR24^{ent-5DS} does not.

There are two additional reasons to question KAR₁ as a KAI2 ligand. First, KAR₁ has been crystallized in complex with KAR-responsive KAI2 proteins from *A. thaliana* (AtKAI2) and the parasitic plant *Striga hermonthica* (ShKAI2iB) (39, 42). Although these proteins have highly similar structures, the KAR₁ molecules have very different orientations in their ligand-binding pockets. Thus, it is unclear which structure, if either, correctly shows KAR₁ binding to the receptor. Notably, neither KAI2 structure captures a substantial conformational change compared to the unbound apo-protein. Second, KAI2 is an extant representative of the evolutionary ancestor of D14. SL perception evolved again more recently in a clade of KAI2 paralogs that emerged in the parasitic Orobanchaceae (12, 49, 50). In both D14 and SL-responsive KAI2d proteins in parasites, the mechanism of SL perception involves hydrolysis of SL and covalent attachment of the cleaved butenolide ring to the His residue in the catalytic triad (13, 14, 47). The triad is essential for KAI2 activity, and KAI2 hydrolyzes GR24^{ent-5DS} in vitro (25, 29). Although it has not yet been reported whether *Arabidopsis* KAI2 signals after forming a covalently linked intermediate molecule (CLIM) from GR24^{ent-5DS}, as D14 and KAI2d proteins do with GR24^{5DS}, the most parsimonious explanation is that the hydrolysis-based signaling mechanism is conserved. If so, it is unclear how KARs may activate KAI2, as the butenolide ring in KARs cannot be cleaved through the same mechanism.

These observations led us and others to hypothesize that KAR₁ must be modified in vivo before it can be recognized by KAI2 (29, 43). Here we show support for this hypothesis that emerged unexpectedly during a reverse genetic study of KAR-RIKIN-UP-REGULATED F-BOX1 (KUF1)/SKP1/ASK-interacting protein 25 (SKIP25). *KUF1/SKIP25* (Atlg31350) is a transcriptional marker of KAR/KL signaling that was first identified among 121 transcripts up-regulated by KAR₁ treatment in a microarray analysis of primary dormant *A. thaliana* seed (5). *KUF1* was later shown to be induced by KAR treatment in seedlings as well (5, 9, 12, 19, 20). Up-regulation of *KUF1* by KAR₁ in *Arabidopsis* requires KAI2 and MAX2. Furthermore, *KUF1* transcripts are reduced in *kai2* and *max2* mutants, and increased in *smxl1 smxl2* (5, 9, 12, 20, 35, 51, 52), which have inactive and constitutive KAR/KL signaling pathway activities, respectively. *KUF1* transcripts are also induced by *rac*-GR24. This response is partially mediated by D14 (12, 53). However, *KUF1* expression is normal in the *d14* mutant, suggesting that *KUF1* is not regulated by endogenous SL signaling. Instead,

the response to exogenous GR24 is likely due to D14 cross-talk with SMXL2 and/or SMAX1 (23). Although *KUF1* expression is up-regulated in *smax1 smxl2* seedlings, it is the same as wild type in *smxl6 smxl7 smxl8*. Furthermore, *KUF1* expression in *smax1 smxl2* is not further affected by treatments that activate D14 (23) (*SI Appendix, Fig. S1*). Therefore, *KUF1* up-regulation is a specific consequence of SMAX1 and SMXL2 degradation, which is typically caused by KAR/KL signaling through KAI2-SCF^{MAX2}. Here we present evidence that this transcriptional response creates a negative feedback loop that putatively regulates the conversion of KAR₁ into a bioactive signal and KL biosynthesis.

Results

Loss of *KUF1* Causes Constitutive KAR/KL Responses in Seedlings. *KUF1* is predicted to have an N-terminal F-box domain, which mediates association with Skp1 in an SCF complex. Prior yeast two-hybrid screens found putative interactions between *KUF1* and the *Arabidopsis* Skp1 proteins ASK1, ASK2, and ASK18 (54, 55). Consistent with these results, we observed F-box domain-dependent interactions between *KUF1* and ASK1 in directed yeast two-hybrid assays (*SI Appendix, Fig. S2A*). This suggests that *KUF1* is a functional F-box protein. UniProt also predicts that *KUF1* has five C-terminal Kelch repeats, which are likely to mediate protein-protein interactions with downstream targets. However, a de novo structural prediction by AlphaFold indicates that *KUF1* may have a six-bladed rather than five-bladed β -propeller structure (*SI Appendix, Fig. S2B*) (56).

We hypothesized that *KUF1* may have a role in activating downstream growth responses to KAR/KL. To investigate this idea, we used an egg cell-specific promoter-controlled CRISPR-Cas9 system (57) to introduce loss-of-function mutations in *KUF1*. Two sites in *KUF1* were targeted simultaneously. We identified a 200-bp deletion between these sites. This allele, *kuf1-1*, is likely to be null, as it causes a translational frameshift that retains only the first 36 amino acids (aa) of the 395-aa protein (Fig. 1A). Contrary to our expectations, *kuf1-1* seedlings grown under continuous red light had reduced hypocotyl elongation and enlarged cotyledons, similar to *smax1* and KAR-treated wild-type (Col-0) seedlings (Fig. 1B). The *kuf1-1* (hereafter, *kuf1*) hypocotyl phenotype is recessive and was rescued by introduction of a wild-type *KUF1p::KUF1* transgene (Fig. 1B and *SI Appendix, Fig. S3*).

To determine whether *kuf1* and *smax1* shared more than morphological similarities, we investigated the expression of transcriptional markers of KAR/KL response in *kuf1* seedlings grown under red light. *D14-LIKE2 (DLK2)*, *B-BOX DOMAIN PROTEIN 20/SALT TOLERANCE HOMOLOG 7/bzr1-1D SUPPRESSOR (BBX20/STH7/BZS1)*, and *SMAX1-LIKE 2 (SMXL2)* are positively regulated by KAR/KL signaling, whereas *INDOLE-3-ACETIC ACID 6 (IAA6)* is negatively regulated by KAR/KL signaling (5, 12, 19, 23, 29). All four genes were differentially expressed in *kuf1* relative to wild type to a similar or stronger extent than we observed in *smax1* and KAR₁-treated wild-type seedlings (Fig. 1C). KAR₁ treatment of *kuf1* seedlings further enhanced the differential expression of these genes (Fig. 1C). Therefore, *kuf1* has constitutive KAR/KL responses, similar to *smax1*, but remains responsive to KAR₁ treatment. Collectively, the seedling growth and gene expression phenotypes of *kuf1* indicated that *KUF1* inhibits the activity or output of the KAR/KL signaling pathway. This suggested that *KUF1* up-regulation after KAI2-SCF^{MAX2}-mediated

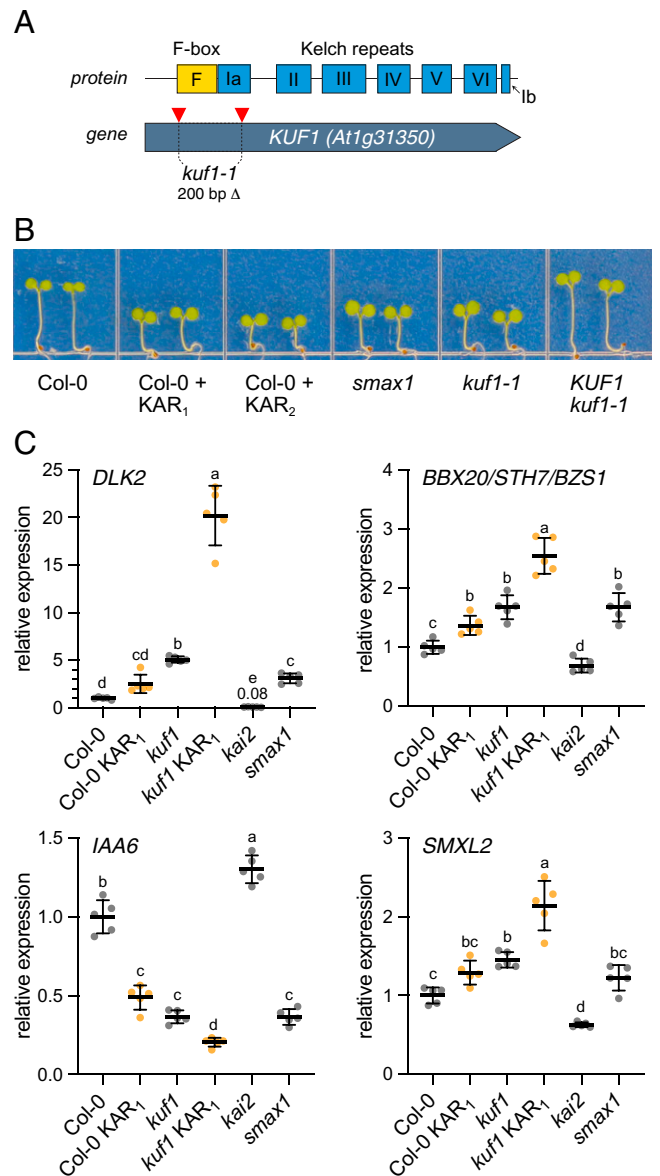


Fig. 1. Isolation of a *kuf1* mutant in *A. thaliana*. (A) Diagram of *KUF1* protein domains and *KUF1* gene structure. Filled arrow, exon; red triangles, gRNA target sites; dashed lines, boundaries of genomic deletion in *kuf1-1*. (B) Seedlings grown 4 d in red light on 0.5× MS medium supplemented with 0.1% (vol/vol) acetone, 1 μM KAR₁, or 1 μM KAR₂. *KUF1 kuf1-1* is a *KUF1p::KUF1 kuf1-1* transgenic rescue line. (C) Expression of *DLK2*, *BBX20/STH7/BZS1*, *IAA6*, and *SMXL2* relative to *CACS* reference transcripts in seedlings grown 4 d in red light on 0.5× MS medium supplemented with 0.1% (vol/vol) acetone (gray) or 1 μM KAR₁ (orange), measured by qRT-PCR. Relative expression values are scaled to Col-0. ($n = 5$ pools of seedlings; mean ± SD). Letters indicate statistical groups, $P < 0.05$, Dunnett's T3 multiple comparisons test.

degradation of SMAX1 and SMXL2 may be part of a negative feedback mechanism.

***KUF1* Acts Upstream of *KAI2* and *MAX2*.** We initially considered three hypotheses to explain *kuf1* phenotypes: 1) *KUF1* may control seedling growth independently of the KAR/KL signaling pathway, 2) *kuf1* may reduce the abundance or activity of SMAX1/SMXL2 proteins independently of KAI2-SCF^{MAX2}, or 3) *kuf1* may enhance SMAX1/SMXL2 degradation by increasing the abundance or activity of KAI2 or MAX2 proteins. The first two hypotheses predict that *kuf1* will at least partially suppress the seedling phenotypes of *kai2* and *max2*, which over

accumulate SMAX1 and SMXL2. To test this, we generated double mutants between *kuf1* and *max2*, *kai2*, and *d14*. We found that *kai2* and *max2*, which have elongated hypocotyls and small cotyledons, are epistatic to *kuf1* (Fig. 2). In contrast, *kuf1 d14* mutant seedlings were similar to *kuf1*. This indicated that a functional KAI2-SCF^{MAX2} signaling mechanism, but not a SL signaling mechanism, is necessary for expression of the *kuf1* phenotype. These results led us to reject the first two hypotheses.

***kuf1* Seedlings Are Hypersensitive to KAR₁ but Not Other KAI2-Mediated Signals.** To investigate the third hypothesis, we first compared the abundance of KAI2 protein in wild-type and *kuf1* seedlings grown under red light. We did not observe a significant difference in KAI2 protein abundance in *kuf1* (Fig. 3A). We also used a ratiometric, dual-fluorescent reporter system to examine how *KUF1* affects KAI2 abundance (22, 58). We transiently coexpressed 35S:*KUF1* or a 35S:*kuf1*Δ mutant with an AtKAI2 ratiometric reporter in *Nicotiana benthamiana* leaves (Fig. 3B). After 3 d, we measured fluorescence from the KAI2-mScarlet-I fusion protein relative to fluorescence from a simultaneously expressed reference protein, Venus. We found that coexpression of wild-type *KUF1* had no effect on the relative abundance of KAI2-mScarlet-I, consistent with our observations in *Arabidopsis* seedlings (Fig. 3B). Therefore, KAI2 is unlikely to be a target of SCF^{KUF1}, which agrees with the prior finding that KAI2 is not polyubiquitinated or degraded after KAR₂ treatment by the 26S proteasome (59).

Nonetheless, the possibilities remained that MAX2 is more abundant in *kuf1*, or that *kuf1* somehow enhances the activity of KAI2 and/or SCF^{MAX2}, putatively resulting in more effective degradation of SMAX1/SMXL2. A reasonable prediction of either case is that *kuf1* seedlings would be hypersensitive to all chemical signals that activate KAI2. Therefore, we examined the seedling growth responses of *kuf1* and *KUF1p::KUF1 kuf1* rescue lines to KAR₁, KAR₂, and *rac-GR24*. As demonstrated by dose-response experiments, the degree to which these treatments inhibit hypocotyl elongation offers a simple and sensitive readout of MAX2-dependent signaling activity (5, 60). We found that KAR responses were altered in *kuf1* seedlings in unexpected ways. Prior studies have consistently shown that *Arabidopsis* is more sensitive to KAR₂ than KAR₁ (4, 5, 8, 59). In *kuf1* seedlings, however, 1 μM KAR₁ caused a stronger reduction in hypocotyl elongation than 1 μM KAR₂ (Fig. 4).

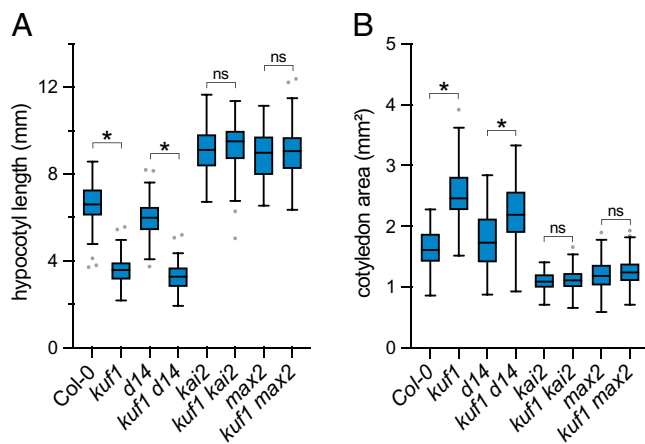


Fig. 2. Epistasis analysis of *kuf1* and KAR/SL signaling mutants. (A) Hypocotyl lengths ($n = 80$) and (B) individual cotyledon areas ($n = 73$ to 78) of seedlings grown 4 d in red light on 0.5× MS medium. Box plots have Tukey whiskers. * $P < 0.01$, Dunnett's T3 multiple comparisons test; ns, not significant.

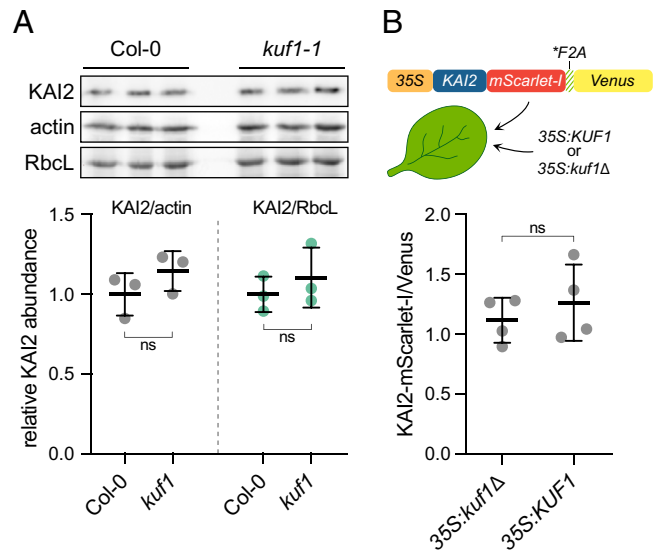


Fig. 3. KAI2 protein abundance under *KUF1* perturbation. (A) Western blot analysis of KAI2 protein abundance in 60 μg total protein extracted from wild-type and *kuf1* *Arabidopsis* seedlings grown 4 d in red light. Actin and Rubisco large subunit (RbcL) were used as loading controls and imaged by Western blot or 2,2,2-trichloroethanol staining, respectively. Relative KAI2 abundance was scaled to Col-0. ($n = 3$ pools of seedlings; mean \pm SD) (B) Ratio of KAI2-mScarlet-I to Venus fluorescence in *N. benthamiana* leaves coinfiltrated 3 d with the pRATIO3212-KAI2 ratiometric reporter plasmid and the 35S-driven overexpression plasmids pGWB402-*kuf1*Δ or pGWB402-*KUF1*. *F2A causes separation of KAI2-mScarlet-I and Venus proteins during translation. The *kuf1*Δ mutation has a deletion that causes premature truncation after the N-terminal 46 aa of *KUF1*. ($n = 4$ leaves, each leaf value is the mean relative fluorescence of six leaf discs; mean \pm SD). ns (not significant), $P > 0.05$, two-tailed unpaired *t* test.

This was mostly due to an enhanced response to KAR₁, as the percentage of growth inhibition by 1 μM KAR₁ on *kuf1* hypocotyls was nearly double that of wild type. However, growth inhibition by 1 μM KAR₂ was also weaker in *kuf1* than wild type. By contrast, the growth response to 1 μM *rac-GR24* was similar in *kuf1* and wild-type hypocotyls (Fig. 4B and *SI Appendix*, Fig. S4A). The unusual KAR responses of *kuf1* hypocotyls were rescued by a wild-type *KUF1* transgene (Fig. 4B and *SI Appendix*, Fig. S4A).

We also compared the ability of KAR₁, KAR₂, and *rac-GR24* to stimulate degradation of a bioluminescent reporter of SMAX1 abundance, SMAX1_{D2}-LUC, in wild-type and *kuf1* backgrounds. This reporter is a translational fusion of the C-terminal D2 domain of SMAX1, which is sufficient for SCF^{MAX2}-induced degradation, to firefly luciferase (22). Supporting the hypocotyl experiment results, KAR₁ caused a stronger decline in SMAX1_{D2}-LUC abundance in *kuf1* seedlings than in wild type during the first 12 h after treatment. By contrast, there was no statistically significant difference ($P > 0.01$) in the response of *kuf1* and wild-type seedlings to either KAR₂ or *rac-GR24* (*SI Appendix*, Fig. S4B).

We found that the hypersensitive response to KAR₁ in *kuf1* seedlings was influenced by the intensity of red light. At 3.8 to 15 μmol m⁻² s⁻¹ red light, the percentage of growth inhibition of *kuf1* hypocotyls by 1 μM KAR₁ was approximately double that observed in wild-type seedlings (*SI Appendix*, Fig. S5A). At higher intensities of red light, the response of wild-type seedlings to KAR₁ increased; under 60 μmol m⁻² s⁻¹ red light the relative responses of wild type and *kuf1* to KAR₁ were the same. In all red light intensities tested, *kuf1* hypocotyls were shorter than wild type (*SI Appendix*, Fig. S5A). In the dark, however, *kuf1* mutants grew to the same length as wild type

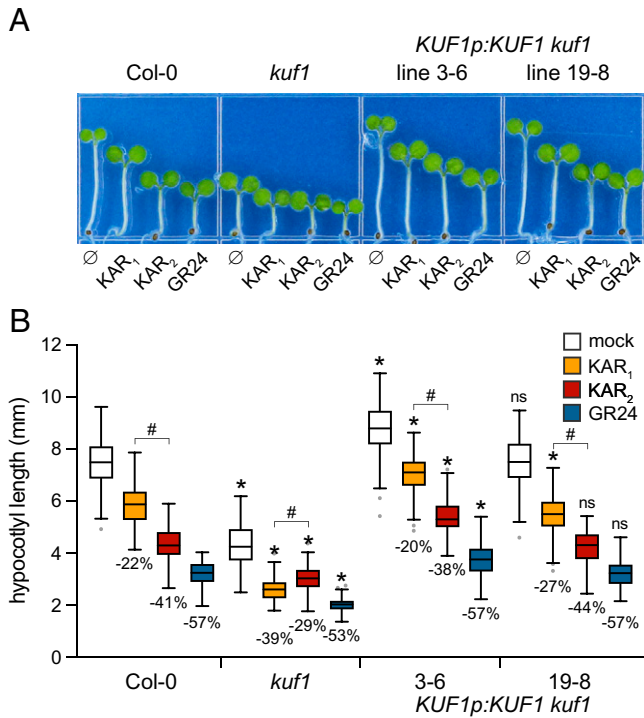


Fig. 4. Hypocotyl elongation response of *kuf1* to KARs and *rac*-GR24. (A) Representative images and (B) hypocotyl lengths of seedlings grown 4 d in red light on 0.5× MS medium supplemented with 0.1% (vol/vol) acetone, 1 μM KAR₁, 1 μM KAR₂, or 1 μM *rac*-GR24. Box plots have Tukey whiskers. Percent growth inhibition relative to the mock-treated control for each genotype is indicated below box plots of experimental treatments. (*n* = 100). **P* < 0.01, Dunnett's multiple comparisons test, compared to Col-0 with the same treatment; ns, not significant. #*P* < 0.01, Dunnett's multiple comparisons test, KAR₁ vs. KAR₂ within the genotype.

and did not show hypocotyl growth responses to KAR₁ or KAR₂ (*SI Appendix, Fig. S5B*). We investigated whether changes in *KUF1* expression might explain the varied effects of KAR₁ on hypocotyl elongation observed under different light fluences. While we found some evidence for higher *KUF1* expression in wild-type seedlings grown in the dark than in red light (*P* = 0.029 to 0.057), there was no clear difference in *KUF1* expression across low to high red light fluences (*SI Appendix, Fig. S5C*). Therefore, other genetic factors likely contribute to KAR₁ responsiveness.

Because KAR₂ and *rac*-GR24 are normally more potent stimulants of KAI2-dependent signaling in *Arabidopsis* seedlings than KAR₁, we reasoned that responses to these signals may appear compressed in *kuf1* if a maximum growth inhibition were approached. That is, *kuf1* might also be hypersensitive to KAR₂ and *rac*-GR24, but an enhanced response cannot be detected if KAI2 activation is already saturated. Therefore, we tested *kuf1* responses to lower concentrations of KAR₂ and *rac*-GR24 (Fig. 5). At all concentrations, KAR₁ caused stronger growth inhibition of *kuf1* hypocotyls than wild type. In contrast, *kuf1* responses to KAR₂ were similar to those of wild type at 100-nM and 300-nM concentrations and less than wild type at 1 μM (Fig. 5A). At all concentrations tested, *kuf1* showed growth responses to *rac*-GR24 that were similar to wild type (Fig. 5B). Notably, we observed in wild-type seedlings that 100 nM *rac*-GR24 caused an equivalent degree of hypocotyl growth inhibition as 1 μM KAR₁ (23% vs. 24%, respectively; Fig. 5A and B). The *kuf1* seedlings showed a wild-type response (25% growth inhibition) to this low concentration of *rac*-GR24, despite having an enhanced response to 1 μM KAR₁

(47% growth inhibition). Therefore, *kuf1* is hypersensitive to KAR₁ but not KAR₂ or *rac*-GR24.

We considered the possibility that the similar responses of *kuf1* and wild-type hypocotyls to *rac*-GR24 could reflect the ability of *rac*-GR24 to activate both KAI2 and D14, whereas KAR₁ only signals through KAI2. This led us to test the *rac*-GR24 responses of *kuf1* seedlings in the absence of signaling contributions from D14. As previously demonstrated, *d14* was less responsive to *rac*-GR24 than wild type (12) (Fig. 5C). However, we found that hypocotyl elongation of *d14* and *kuf1* *d14* seedlings was inhibited to a similar degree by *rac*-GR24 (39% vs. 36%, Fig. 5C). Therefore, the KAI2-SCF^{MAX2} signaling pathway in *kuf1* responds normally to *rac*-GR24.

A Fourth Hypothesis for KUF1 Function. A previous study showed that ~25-fold overexpression of *KAI2* causes *Arabidopsis* seedlings to become hypersensitive to both KAR₂ and *rac*-GR24, but does not impact hypocotyl length in the absence of such treatments (60). In contrast, we observed that 1) *kuf1* is specifically hypersensitive to KAR₁ but not KAR₂ or *rac*-GR24, and 2) *kuf1* affects seedling growth in the absence of treatments in a KAI2-SCF^{MAX2}-dependent manner. This implied that *kuf1* does not increase the overall sensitivity or responsiveness of the KAI2 signaling pathway as proposed by the third hypothesis above, but instead modifies the ability of specific signals to be perceived by KAI2. Therefore, we hypothesized that

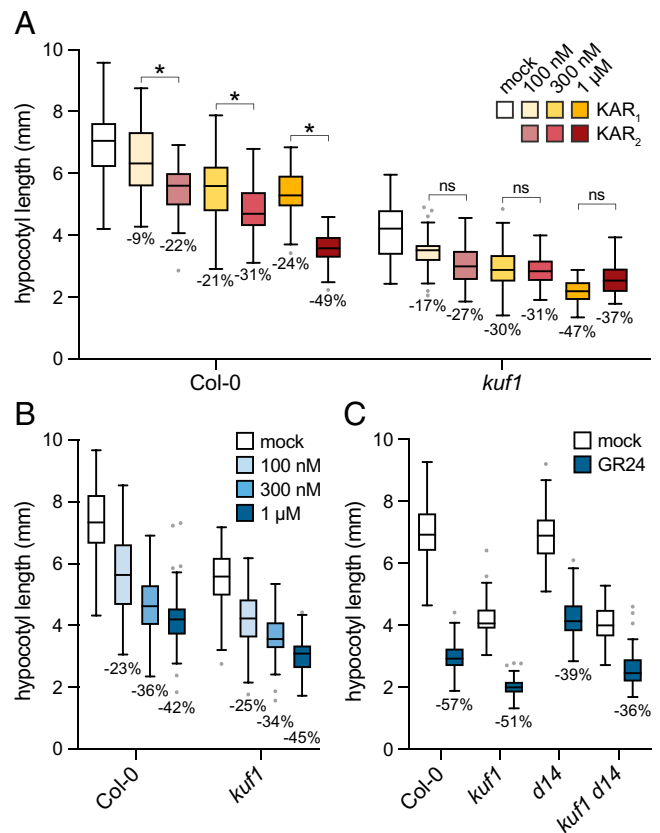


Fig. 5. Response of *kuf1* to low concentrations of KARs and *rac*-GR24. Hypocotyl lengths of wild-type and *kuf1* seedlings grown 4 d in red light on 0.5× MS medium supplemented with 0.1% (vol/vol) acetone, 100 nM, 300 nM, or 1 μM (A) KAR₁ or KAR₂ (*n* = 60), or (B) *rac*-GR24 (*n* = 80). For (A) **P* < 0.01, Tukey's multiple comparisons test; ns, not significant. (C) Hypocotyl lengths of seedlings grown 4 d in red light on 0.5× MS medium supplemented with 0.1% (vol/vol) acetone or 1 μM *rac*-GR24. (*n* = 80). Box plots have Tukey whiskers. Percent growth inhibition relative to the mock-treated control for each genotype is indicated below box plots of experimental treatments.

KUF1 negatively regulates metabolism of KAR₁ into a bioactive signal. In addition, the phenotypes of *kuf1* seedlings are similar to those of *smax1* or KAR-treated wild-type seedlings, suggesting that the KAR/KL signaling pathway is more active than normal (Fig. 1). This could be explained if KUF1 also negatively regulates KL biosynthesis or availability. Such a model would be consistent with the observation that *kuf1* phenotypes are dependent on *MAX2* and *KAI2* (Fig. 2).

KL Abundance Is Likely Increased in *kuf1*. It was not possible for us to directly test whether KL biosynthesis and KAR₁ metabolism are enhanced in *kuf1* because KL and KAR₁ metabolites have not yet been identified. Instead, we used three strategies to indirectly investigate *KUF1* effects on KL levels and KAR₁ metabolism. First, we took advantage of the diversified ligand preferences found among *KAI2* paralogs in root parasitic plants in the Orobanchaceae. A gene from witchweed (*S. hermonthica*), *ShKAI2i*, encodes a subfunctionalized receptor that responds well to KAR₁ and appears to be less sensitive to KL (28, 49). Introducing *ShKAI2i* into an *Arabidopsis kai2* mutant produces seedlings that retain similar morphology to *kai2*. However, the *ShKAI2i kai2* transgenic line is fully responsive to KAR₁ treatment, and the degree of hypocotyl elongation inhibition by KAR₁ is in fact stronger than wild type, indicating that *ShKAI2i* is functional in *Arabidopsis* (28). At a later stage of development, *ShKAI2i* partially rescues the altered rosette morphology of *kai2* mutants grown in short day conditions. Putatively, *ShKAI2i* does not rescue *kai2* seedlings and only partially rescues *kai2* leaf development because it has reduced sensitivity to KL (28). We reasoned that the *ShKAI2i kai2* line may provide a way to test whether KL levels are increased in *kuf1* seedlings. According to our model, loss of *KUF1* should not reduce the hypocotyl elongation of *ShKAI2i kai2* as strongly as it does wild type because *ShKAI2i* would be less sensitive to increased KL abundance than the native *AtKAI2* protein. Responses to KAR₁, however, should be increased by *kuf1* at least as strongly when *ShKAI2i* is the available *KAI2* receptor as when *AtKAI2* is.

To test this, we used CRISPR-Cas9 to recreate the identical 200-bp *kuf1-1* deletion in *ShKAI2i kai2* and its corresponding wild-type ecotype, *Ler*. Similar to what we previously observed in the *Col-0* ecotype, the *kuf1* mutation enhanced the response to KAR₁ treatment in both *Ler* and *ShKAI2i kai2* backgrounds (Fig. 6A). However, under mock-treated conditions—when only endogenous KL is available to seedlings—hypocotyl elongation was reduced by 41% in *kuf1* compared to *Ler* and by only 25% in *kuf1 ShKAI2i kai2* compared to *ShKAI2i kai2* (Fig. 6A). These results are consistent with the idea that KL is increased in *kuf1* mutants, but has a smaller effect on the growth of *ShKAI2i kai2* seedlings than wild type because *ShKAI2i* protein is less able to perceive it than *AtKAI2*.

Second, we compared the abundance of the SMAX1_{D2}-LUC reporter in untreated wild-type and *kuf1* seedlings. We observed lower luminescence in *kuf1* seedlings than in wild type, suggesting reduced abundance of SMAX1_{D2}-LUC and presumably SMAX1, which would be consistent with higher KL levels (Fig. 6B).

Third, we used the ratiometric reporter system to examine how *KUF1* affects SMAX1 abundance and its degradation after KAR₁ treatment (22, 58). We transiently coexpressed 35S:*KUF1* with a SMAX1 ratiometric reporter in *N. benthamiana* leaves for 3 d, treated excised leaf discs with KAR₁, and measured the ratio of SMAX1-mScarlet-I to Venus fluorescence after 16 h. We noted across many experiments that the

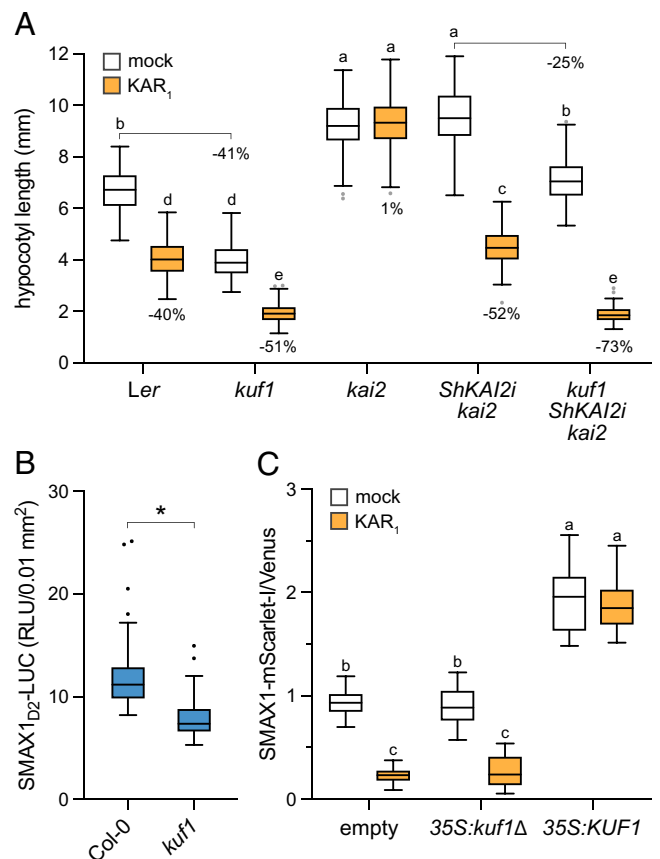


Fig. 6. Indirect tests of *KUF1* effects on KAR and KL metabolism. (A) Hypocotyl lengths of seedlings grown 4 d in red light on 0.5x MS medium supplemented with 0.1% (vol/vol) acetone or 1 μ M KAR₁. The *kuf1* allele is identical to *kuf1-1* but it was made in the *Ler* ecotype and the CRISPR-Cas9 T-DNA has not been removed. *ShKAI2i kai2* expresses *KAI2i* from *S. hermonthica* under control of an *Arabidopsis KAI2* promoter in the *kai2-2* mutant background. Percent growth inhibition relative to the mock-treated control for each genotype is indicated below box plots of KAR₁ treatments. Percent growth inhibition due to *kuf1* is indicated above box plots. ($n = 80$ to 100) (B) Arbitrary relative luminescence units of 9-d-old SMAX1_{D2}-LUC *Col-0* and *kuf1* seedlings grown in 16 h white light:8 h dark, normalized to each seedling's leaf and cotyledon surface area. Wild-type and *kuf1* leaf/cotyledon surface areas were not different ($P > 0.05$). ($n = 36$ seedlings) * $P < 0.01$, Student's two-tailed t test. (C) Ratio of SMAX1-mScarlet-I to Venus fluorescence in *N. benthamiana* leaves coinfiltrated 3 d with the pRATIO1212-SMAX1 ratiometric reporter plasmid and the overexpression plasmids pGWB402 (empty), pGWB402-*kuf1Δ*, or pGWB402-*KUF1*, after a 16-h treatment with 0.02% (vol/vol) acetone or 10 μ M KAR₁. The *kuf1Δ* mutation has a deletion that causes premature truncation after the N-terminal 46 aa of *KUF1*. ($n = 14$ to 18). Letters indicate statistical groups, $P < 0.01$, Tukey's multiple comparisons test. Box plots have Tukey whiskers.

abundance of the SMAX1 reporter was consistently higher in mock-treated leaves coexpressing wild-type *KUF1* compared to those coexpressing an empty vector or a *kuf1Δ* frameshift allele (Fig. 6C and *SI Appendix*, Fig. S6). This observation is consistent with the hypothesis that *KUF1* overexpression blocks production of KL, thus promoting stabilization of SMAX1.

We also found that coexpression of wild-type *KUF1* prevented KAR₁-induced degradation of the SMAX1 reporter (Fig. 6C). This led us to test whether *KUF1* overexpression impacts the ability of other treatments to trigger SMAX1 degradation. In wild-type *N. benthamiana* plants, *KUF1* overexpression blocked degradation of the SMAX1 reporter by KAR₂ as well as KAR₁, but *rac-GR24* was still active (*SI Appendix*, Fig. S6A). To determine whether the remaining *rac-GR24* response was mediated by D14 or *KAI2*, we also performed the

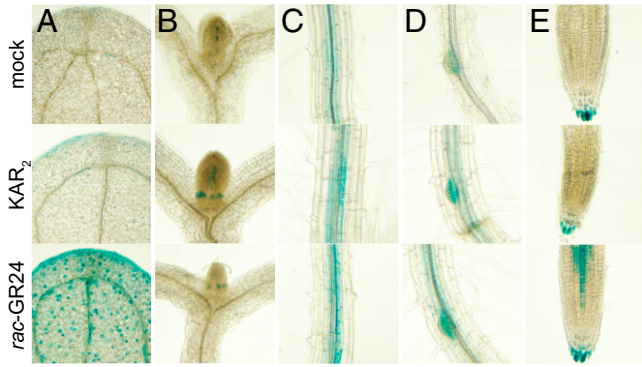


Fig. 7. *KUF1* expression patterns in *Arabidopsis* seedlings. Representative micrographs of β -glucuronidase staining (blue) in (A) cotyledons, (B) shoot apices, (C) mature root cells, (D) lateral root primordia, and (E) primary root tips of *KUF1p:GUS* seedlings grown 4 d in red light on 0.5 \times MS supplemented with 0.1% (vol/vol) acetone, 1 μ M *KAR*₂, or 1 μ M *rac-GR24*.

experiment in an *Nbd14a,b* double mutant that has loss-of-function mutations in the two *D14* homoeologs in *N. benthamiana* (61). We found that the *SMAX1* reporter was not degraded in response to *KAR*₁, *KAR*₂, or *rac-GR24* in *Nbd14a,b* leaves when *KUF1* was overexpressed (SI Appendix, Fig. S6B). This suggests that *KUF1* overexpression inhibits all *KAI2*-mediated degradation of *SMAX1* in *N. benthamiana*, which was not expected from the characterization of *Arabidopsis kuf1*. This effect is not due to the loss of *KAI2* protein (Fig. 3B) and is at the moment difficult to explain given that *GR24* should not require metabolism to activate *KAI2*.

Are *KUF1* Expression Patterns a Cause or an Effect of KL Distribution? Because *KUF1* expression is an output of *KAR/ KL* signaling, its expression pattern in plants may reveal where *KL* is most abundant, *KAI2* is most active, and/or *SMAX1* and *SMXL2* abundance is lowest. An alternative, nonmutually exclusive possibility is that *KUF1* expression patterns are imposed in certain tissues or by other cellular pathways as a way to restrict *KL* abundance and *KAI2* activity. We generated transcriptional reporters for *KUF1* by using the $-2,967$ -bp region upstream of *KUF1* to drive expression of the β -glucuronidase (*GUS*) reporter. This upstream region provides appropriate *cis*-regulation for *KUF1* to rescue the *kuf1* mutant (Fig. 4 and SI Appendix, Fig. S3).

We found that in seedlings, the *KUF1* promoter region drives *GUS* expression in the root cap, newly emerged leaves, and mature vasculature in the root, but not in the differentiation or elongation zones of the root. *GUS* activity was also generally lacking in the hypocotyl (Fig. 7). In some strongly expressing lines, we observed *GUS* activity in the stomata of cotyledons. In 5-wk-old adult plants, the *KUF1* promoter was active in leaves, rosette axillary buds, sepals, and anthers (SI Appendix, Fig. S7). We investigated whether *KUF1* expression is limited to specific tissues in seedlings because of ligand (i.e., *KL*) availability or because only some tissues are competent to respond to *KAI2* agonists. These possibilities may be distinguished, respectively, by whether *KAR* and *rac-GR24* treatments increase the spatial distribution or only the intensity of *KUF1* expression. We observed that *KAR*₂ and *rac-GR24* tended to intensify, rather than expand, the regions with *GUS* activity in 5-d-old seedlings grown in red light. Therefore, the ability to express *KUF1*, or *KAI2-SCF*^{MAX2} signaling itself, may be limited to specific tissues. Interestingly, the expression pattern of *KUF1* corresponds well with that of *SMAX1* (34).

***KUF1* Negatively Regulates *KAI2*-Mediated Root Hair Development.** The expression of *KUF1* in roots led us to consider whether it has a role in root development. Because *Arabidopsis* root hair density and elongation are positively regulated by the *KAR/ KL* pathway, we investigated the effects of *kuf1* on root hair growth (37). As previously demonstrated, we observed that *KAR*₁ and *KAR*₂ increased root hair density and elongation in a *KAI2*- and *MAX2*-dependent manner (Fig. 8). Moreover, *kai2* and *max2* mutants showed reduced root hair density and elongation under mock treatment. We found that *kuf1* seedlings have increased root hair density and root hair elongation compared to wild type under mock treatment, which is consistent with a constitutive *KAR/ KL* response (Fig. 8). This phenotype was rescued by *KUF1p:KUF1*. In addition, *KAR*₁ enhanced root hair density more than *KAR*₂ in *kuf1* but not wild-type roots, similarly to our observations of *KAR*₁ hypersensitivity in *kuf1* hypocotyls (Fig. 8A). Therefore, *KUF1* imposes negative feedback regulation on multiple developmental processes regulated by *KAI2-SCF*^{MAX2} in *Arabidopsis*.

Discussion

KUF1 is one of ~ 103 F-box proteins with C-terminal Kelch repeats in *A. thaliana*. It is the sole member of one of eight “superstable” clades of F-box Kelch genes that have been defined based on having orthologs in eudicots *A. thaliana*, *Populus trichocarpa*, and *Vitis vinifera*; the monocots *Oryza*

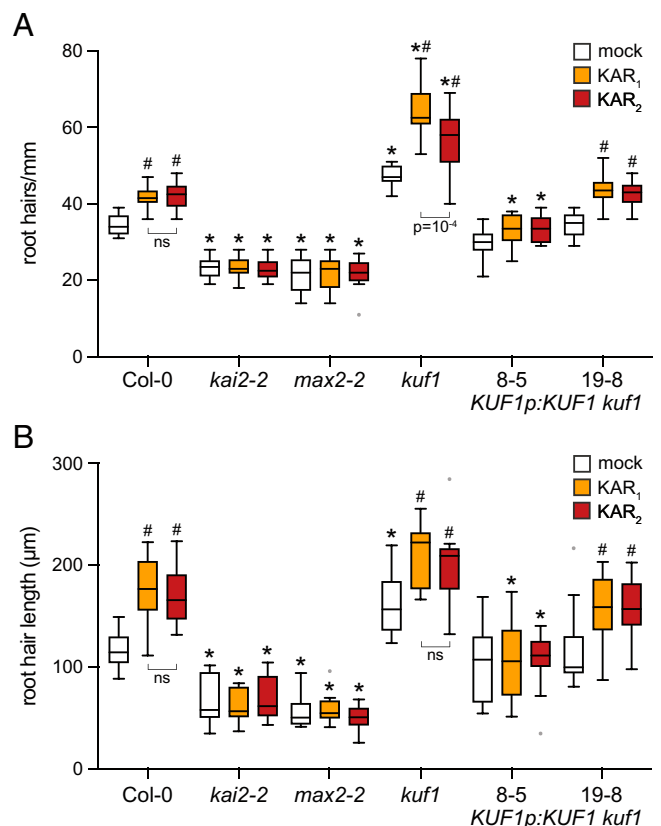


Fig. 8. Root hair density and elongation in *kuf1*. (A) Root hair density ($n = 10$) and (B) root hair length ($n = 10$ roots, represented by average of 10 root hairs from each) of 5-d-old seedlings grown vertically in white light ($120 \mu\text{mol m}^{-2} \text{s}^{-1}$) on 0.5 \times MS medium supplemented with 1% (wt/vol) sucrose and 0.07% (vol/vol) methanol, 1 μ M *KAR*₁, or 1 μ M *KAR*₂. The *kai2-2* allele was introgressed into the Col-0 background. Box plots have Tukey whiskers. * $P < 0.01$, Dunnett’s multiple comparisons test, compared to Col-0 with the same treatment. # $P < 0.01$, Dunnett’s multiple comparisons test, compared to mock treatment within the genotype. ns, not significant.

sativa and *Sorghum bicolor*; the lycophyte *Selaginella moellendorffii*; and the bryophyte *Physcomitrium patens* (62). These superstable F-box genes are under purifying selection and therefore have been proposed to carry out developmental or physiological functions that are conserved in land plants (62). Here we identified roles for *KUF1* in *Arabidopsis* seedling and root hair development that likely arise from its molecular function as a negative regulator of responses to KAR₁ and KL. This raises the possibility that *KUF1* may affect other aspects of plant growth and development regulated by KAR/KL signaling such as seed germination, drought tolerance, and symbiotic interactions with arbuscular mycorrhizal fungi.

It is possible that up-regulation of *KUF1* after activation of SCF^{MAX2}-regulated signaling pathways is a widely conserved response in land plants. In *P. patens*, at least one of the four *KUF1* orthologs (Pp3c2_34130v3.1) shows induced expression following *rac*-GR24 treatment and is down-regulated in a *Ppmax2* mutant. Induction of *KUF1* by *rac*-GR24 is dependent on *PpMAX2*, at least when the moss is grown in the light (63). In *O. sativa* (rice), *OsKUF1* (LOC_Os06g49750) is up-regulated severalfold in *smx1* and is also induced by KAR₁ and GR24^{ent-5DS} in a KAI2/D14L-dependent manner (64). In *Pisum sativum* (pea) buds, *PskUF1* (Psat2g143160) is reported in a preprint to be up-regulated by *rac*-GR24 in the SL-deficient *rms1/ccd8* and *rms5/ccd7* backgrounds, by GR24^{5DS} in *rms1/ccd8*, and, unexpectedly, by KAR₁ in *rms4/max2* only (65). In *Lactuca sativa* (lettuce), we have found that at least one of its three *KUF1* homologs shows increased expression in achenes imbibed for 6 h with 1 μM KAR₁ or KAR₂ relative to mock treatment (SI Appendix, Fig. S8).

The *kuf1* loss-of-function mutant shows several developmental and transcriptional phenotypes that are consistent with hyperactive KAR/KL signaling. We considered several hypotheses for how *KUF1* may reduce the effects of the KAR/KL pathway on plant growth and development. Although *KUF1* expression is negatively regulated by *SMAX1* and *SMXL2*, epistasis analysis demonstrated that *KUF1* acts upstream of *KAI2* and *MAX2*. This suggests a negative feedback loop. We also observed that *kuf1* seedlings are hypersensitive to KAR₁ but not *rac*-GR24. Therefore, *KUF1* affects the ability of different molecules to be perceived by *KAI2*. This leads us to hypothesize that *KUF1* negatively regulates metabolism of KAR₁ into a bioactive ligand of *KAI2* (Fig. 9). Because *kuf1* phenotypes under control conditions are similar to *smx1* and KAR-treated wild-type seedlings, we further propose that *KUF1* negatively regulates biosynthesis of the unknown endogenous *KAI2* ligand, KL. One way this could occur is through SCF^{KUF1}-mediated polyubiquitylation and proteolysis of an enzyme(s) that metabolizes KAR₁ and/or KL. Indeed, if there were an enzyme that carried out both KAR₁ metabolism and KL biosynthesis, it could help explain the potential for KAR response in nonfire following angiosperms such as *Arabidopsis*, for which the selective pressure to maintain a KAR response mechanism is not obvious. Alternatively, negative regulation of a KAR₁/KL-metabolizing enzyme(s) by *KUF1* could be less direct, such as by modulating the abundance of a transcription factor(s) that controls expression of the enzyme(s) or production of an enzyme cofactor. In this model, up-regulation of *KUF1* expression in response to SCF^{MAX2}-mediated degradation of *SMAX1*/*SMXL2* represents a negative feedback mechanism for KL homeostasis that occurs through proteolysis rather than transcriptional repression (Fig. 9).

Our results raise the question of why *rac*-GR24 responses remain normal in *kuf1*. We propose that *rac*-GR24, or more specifically the GR24^{ent-5DS} stereoisomer, is a “ready-to-go”

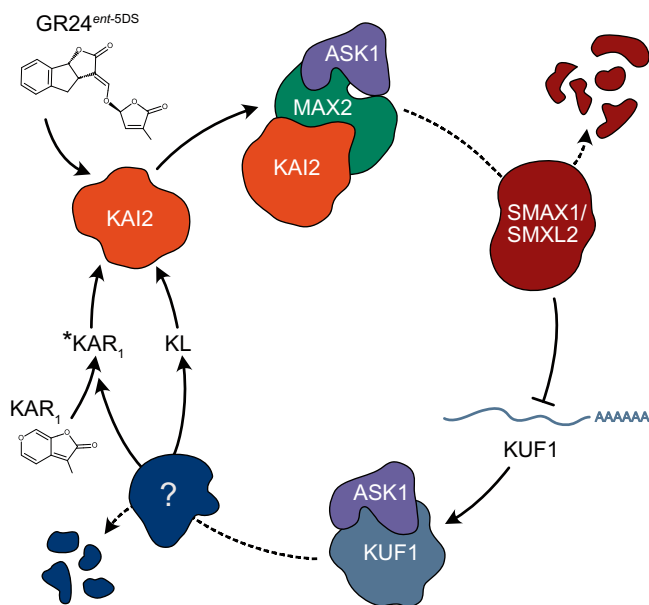


Fig. 9. Model of a *KUF1*-mediated negative feedback loop. Activation of *KAI2* by an unknown endogenous ligand (KL), a putative KAR₁ metabolite (*KAR₁), or GR24^{ent-5DS} triggers its association with SCF^{MAX2} and *SMAX1*/*SMXL2*. *SMAX1*/*SMXL2* proteins are polyubiquitinated and degraded by the 26S proteasome, causing an increase in *KUF1* transcripts. *KUF1* likely acts within an SCF-type E3 ubiquitin ligase complex to target (an) unknown protein(s) for polyubiquitination and proteasomal degradation. The *KUF1* target(s) positively regulate(s) KL biosynthesis and conversion of KAR₁ into a bioactive signal. Thus, up-regulation of *KUF1* following *SMAX1*/*SMXL2* degradation dampens the plant's capacity to produce additional ligands for *KAI2* but does not affect its ability to respond to GR24^{ent-5DS}. For simplicity, components of the E3 ubiquitin ligase complex other than *Arabidopsis* Skp1 (*ASK1*) are not shown.

ligand that is able to be recognized directly by *KAI2* without metabolite. This is supported by the observation of thermal stability shifts in *KAI2* after GR24^{ent-5DS} treatment in DSF assays and by yeast two-hybrid interactions between *KAI2* and *SMAX1* in the presence of *rac*-GR24 and GR24^{ent-5DS} (8, 22, 29). In addition, GR24 has a hydrolyzable butenolide D-ring that KARs lack, which has been shown to be important for signaling activity in many D14 agonists. KAR₂ responses in *kuf1*, which are not enhanced and even seem to be decreased under 1-μM treatments, are difficult to explain at this time. Presumably KAR₂ also requires metabolism by plants, as it is inactive on *KAI2* in DSF and yeast two-hybrid assays, but this might be carried out by a protein or mechanism not regulated by *KUF1*. Different responses to KAR₁ and KAR₂ also occur in *Lottus japonicus*, where both compounds affect hypocotyls but only KAR₁ affects root growth (66). Because the receptor that mediates KAR₂ responses, LjKAI2a, is active in both hypocotyls and roots, tissue-specific metabolism of KAR₂ that is independent of KAR₁ metabolism might explain this phenomenon.

A notable weakness of the proposed model (Fig. 9) is the inability to directly evaluate KL abundance. Until KL is identified, alternative explanations of these data that we have not considered remain possible. One observation that is currently difficult to reconcile with the model is the effect of *KUF1* overexpression on *SMAX1* degradation in *N. benthamiana*, which blocks responses to KAR₁, KAR₂, and *rac*-GR24 rather than just KAR₁. One possibility is that a metabolic precursor of KL overaccumulates when *KUF1* is overexpressed that competitively inhibits activation of *KAI2* by other molecules.

It is notable that although *kuf1* has a shortened hypocotyl phenotype, *KUF1* expression was either absent or very low in *Arabidopsis* hypocotyls compared to other seedling tissues. This

suggests that *KUF1* effects on hypocotyl elongation are not locally mediated. Similarly, another transcriptional marker of KAR/KL signaling, B-box domain protein BBX20/STH7, regulates hypocotyl elongation but has very low expression in seedling hypocotyls compared to other tissues (52). There are a number of possibilities for how KUF1 could act at a distance to affect hypocotyl elongation, including direct or indirect control of a mobile signal or protein. For example, KL may be transported from its site(s) of synthesis to act in other tissues. Auxin is another attractive candidate for a mobile signal. KAI2 remodels auxin distribution in seedlings during photomorphogenesis, putatively by controlling the abundance of the auxin efflux carriers PIN1, PIN3, and PIN7 at the plasma membrane. This in turn influences hypocotyl elongation and root development (67).

An outstanding goal for the SL and KAR field is the identification of KL, which will give insights into the function of KAI2 as well as the evolutionary history of the SL and KAR signaling pathways. This characterization of KUF1 reveals strategies to achieve this goal. First, *kuf1* tissues may provide a more abundant source of KL than wild type for bioassay-guided fractionation approaches to isolate purified KL. Second, identification of the protein(s) targeted for degradation by SCF^{KUF1} should provide insights into how KL and KAR₁ metabolism occur and may even uncover enzymes that are directly involved in KL biosynthesis. Biochemical approaches to identify proteins that interact with KUF1 and/or genetic approaches to identify *kuf1* suppressors may prove fruitful for discovering these targets.

Materials and Methods

Materials. *A. thaliana* alleles in the Col-0 ecotype used here were *d14-1*, *htl-3* ("kai2" here for clarity), *d14-1 htl-3*, *smx1-2*, *max2-1*, *max2-2*, and *smx1-2 smxl2-1* (12, 19, 20, 41, 68). The *kai2-2* allele (*Ler* ecotype) and the *ShKAI2i kai2-2* transgenic line are also described previously (12, 49). *SMAX1_{D2}-LUC kuf1* was derived through crossing *kuf1-1* into the previously described *UBQ10:S-MAX1_{D2}-LUC2-*F2A-mScarlet-1* transgenic *Arabidopsis* line (22). Fig. 8 uses a *kai2-2* allele backcrossed six times into the Col-0 background. KAR₁, KAR₂, and *rac-GR24* were synthesized and provided by Gavin Flematti and Adrian Scaffidi, University of Western Australia, Perth, Australia. KAR and *rac-GR24* stocks were prepared in acetone, stored at -20°C , and freshly diluted before use. Oligonucleotide primer sequences for cloning, genotyping, and expression analysis are described in *SI Appendix, Table S1*. Additional detailed methods are described in *SI Appendix, Materials and Methods*.

Isolation and Rescue of *kuf1*. Based on cDNA and expressed sequence tag support, the gene model At1g31350.1 (395 aa) was used for *KUF1* instead of At1g31350.2 (431 aa). Two *KUF1* sites, 5'-GAAACTCCGCTTAATCGAAGG-3' and 5'-CGGTTTATGTGTTCAACCCGG-3' (protospacer adjacent motif underlined), with a minimum mismatch of five nucleotides (nt) to the next closest genomic

sequence were selected from the CRISPR-PLANT gRNA database for gene editing by CRISPR-Cas9 (69). Both gRNA sequences were introduced into pHEE401E through GoldenGate cloning as previously described, but with Q5 DNA polymerase (New England Biolabs) during cassette amplification steps (57, 70). *Arabidopsis* was transformed by floral dip with Sanger sequence-verified pHEE401E-KUF1. Seed was screened on $0.5\times$ Murashige-Skoog (MS) media with hygromycin B (20 $\mu\text{g}/\text{mL}$) to identify T₁ plants. The *kuf1-1* allele (200-bp deletion between +107 and +307 of the coding sequence) was identified by PCR (*SI Appendix, Table S1*) and verified by Sanger sequencing. The *kuf1-1* allele generated in Col-0 and *Ler* backgrounds was identical at the nucleotide level. The pHEE401E-KUF1 T-DNA was removed from the *kuf1-1* allele in Col-0 ecotype through segregation, but was not removed in the *Ler* ecotype *kuf1* lines. To rescue *kuf1*, a genomic KUF1 sequence (from $-2,967$ upstream of the translational start codon to the stop codon) was cloned into pDONR221A, a Gateway entry vector modified to have ampicillin resistance), sequence-verified, and transferred into pGWB501 (71) with LR clonase II (Invitrogen). The resulting pGWB501-KUF1p:KUF1 was introduced into *kuf1-1* by floral dip. Homozygous, single-insertion transgenic lines were characterized.

Seedling Growth Assays. Surface-sterilized seeds were plated on solid $0.5\times$ MS media supplemented with KARs, *rac-GR24*, or an equivalent volume of solvent as indicated. Seeds were stratified in the dark for 3 d at 4°C , then moved to a HiPoint DCI-700 LED Z4 growth chamber to grow at 21°C under white light ($150\ \mu\text{mol}\ \text{m}^{-2}\ \text{s}^{-1}$) for 3 h, dark for 21 h, and red light ($30\ \mu\text{mol}\ \text{m}^{-2}\ \text{s}^{-1}$ unless noted otherwise) for 4 d. Multiple fluences were simultaneously achieved with foil-lined boxes covered with neutral density gel sheets (Lee filters 209, 210, 211, 299) placed under $60\ \mu\text{mol}\ \text{m}^{-2}\ \text{s}^{-1}$ red light. Hypocotyl lengths of photographed seedlings were measured with ImageJ (NIH). Cotyledon surface areas were measured in ImageJ from photographs of seedlings mounted in water on glass slides.

Statistical Analysis. Statistical analysis was performed in Prism 9 (GraphPad). Post hoc statistical comparisons were performed after ANOVA or two-way ANOVA. Box plots show the median, 25th percentile, and 75th percentile. Tukey whiskers on box plots extend 1.5 times the interquartile range beyond the 25th/75th percentile up to the minimum/maximum value in the dataset. Outlier data beyond Tukey whiskers are shown as individual points.

Data Availability. All study data are included in the article and/or *SI Appendix*.

ACKNOWLEDGMENTS. Funding was provided by the NSF to D.C.N. (IOS-1856741) and J.M.G. (IOS-1856452); by the Australian Research Council to M.T.W. (DP21013078), and the Emmy Noether program (GU1423/1-1) of the Deutsche Forschungsgemeinschaft (to C.G.). We thank Dr. Gavin Flematti and Dr. Adrian Scaffidi (University of Western Australia) for graciously supplying KARs and *rac-GR24*.

Author affiliations: ^aDepartment of Botany and Plant Sciences, University of California, Riverside, CA 92521; ^bPlant Genetics, TUM School of Life Sciences, Technical University of Munich, Freising, 85354 Germany; ^cSchool of Molecular Sciences, University of Western Australia, Perth, WA 6009, Australia; and ^dDepartment of Molecular, Cellular, and Developmental Biology, Yale University, New Haven, CT 06511

- D. C. Nelson, G. R. Flematti, E. L. Ghisalberti, K. W. Dixon, S. M. Smith, Regulation of seed germination and seedling growth by chemical signals from burning vegetation. *Annu. Rev. Plant Biol.* **63**, 107–130 (2012).
- G. R. Flematti, E. L. Ghisalberti, K. W. Dixon, R. D. Trengove, A compound from smoke that promotes seed germination. *Science* **305**, 977 (2004).
- G. R. Flematti, E. L. Ghisalberti, K. W. Dixon, R. D. Trengove, Identification of alkyl substituted 2H-furo[2,3-c]pyran-2-ones as germination stimulants present in smoke. *J. Agric. Food Chem.* **57**, 9475–9480 (2009).
- D. C. Nelson *et al.*, Karrikins discovered in smoke trigger *Arabidopsis* seed germination by a mechanism requiring gibberellic acid synthesis and light. *Plant Physiol.* **149**, 863–873 (2009).
- D. C. Nelson *et al.*, Karrikins enhance light responses during germination and seedling development in *Arabidopsis thaliana*. *Proc. Natl. Acad. Sci. U.S.A.* **107**, 7095–7100 (2010).
- M. G. Kulkarni, M. E. Light, J. Van Staden, Plant-derived smoke: Old technology with possibilities for economic applications in agriculture and horticulture. *S. Afr. J. Bot.* **77**, 972–979 (2011).
- M. Antala, O. Sytar, A. Rastogi, M. Brestic, Potential of karrikins as novel plant growth regulators in agriculture. *Plants* **9**, 43 (2019).
- Y. K. Sun *et al.*, Divergent receptor proteins confer responses to different karrikins in two ephemeral weeds. *Nat. Commun.* **11**, 1264 (2020).
- D. C. Nelson *et al.*, F-box protein MAX2 has dual roles in karrikin and strigolactone signaling in *Arabidopsis thaliana*. *Proc. Natl. Acad. Sci. U.S.A.* **108**, 8897–8902 (2011).
- V. Gomez-Roldan *et al.*, Strigolactone inhibition of shoot branching. *Nature* **455**, 189–194 (2008).
- M. Umehara *et al.*, Inhibition of shoot branching by new terpenoid plant hormones. *Nature* **455**, 195–200 (2008).
- M. T. Waters *et al.*, Specialisation within the DWARF14 protein family confers distinct responses to karrikins and strigolactones in *Arabidopsis*. *Development* **139**, 1285–1295 (2012).
- R. Yao *et al.*, DWARF14 is a non-canonical hormone receptor for strigolactone. *Nature* **536**, 469–473 (2016).
- A. de Saint Germain *et al.*, An histidine covalent receptor and butenolide complex mediates strigolactone perception. *Nat. Chem. Biol.* **12**, 787–794 (2016).
- Y. Seto *et al.*, Strigolactone perception and deactivation by a hydrolase receptor DWARF14. *Nat. Commun.* **10**, 191 (2019).
- L. Jiang *et al.*, DWARF 53 acts as a repressor of strigolactone signalling in rice. *Nature* **504**, 401–405 (2013).
- F. Zhou *et al.*, D14-SCF(D3)-dependent degradation of D53 regulates strigolactone signalling. *Nature* **504**, 406–410 (2013).

18. L. Wang *et al.*, Strigolactone signaling in Arabidopsis regulates shoot development by targeting D53-like SMXL repressor proteins for ubiquitination and degradation. *Plant Cell* **27**, 3128–3142 (2015).
19. J. P. Stanga, S. M. Smith, W. R. Briggs, D. C. Nelson, SUPPRESSOR OF MORE AXILLARY GROWTH2 1 controls seed germination and seedling development in Arabidopsis. *Plant Physiol.* **163**, 318–330 (2013).
20. J. P. Stanga, N. Morffy, D. C. Nelson, Functional redundancy in the control of seedling growth by the karrikin signaling pathway. *Planta* **243**, 1397–1406 (2016).
21. M. T. Waters, C. Gutjahr, T. Bennett, D. C. Nelson, Strigolactone signaling and evolution. *Annu. Rev. Plant Biol.* **68**, 291–322 (2017).
22. A. Khosla *et al.*, Structure-function analysis of SMAX1 reveals domains that mediate its karrikin-induced proteolysis and interaction with the receptor KAI2. *Plant Cell* **32**, 2639–2659 (2020).
23. L. Wang *et al.*, Strigolactone and karrikin signaling pathways elicit ubiquitination and proteolysis of SMXL2 to regulate hypocotyl elongation in Arabidopsis. *Plant Cell* **32**, 2251–2270 (2020).
24. A. Scaffidi *et al.*, Strigolactone hormones and their stereoisomers signal through two related receptor proteins to induce different physiological responses in Arabidopsis. *Plant Physiol.* **165**, 1221–1232 (2014).
25. G. R. Flematti, A. Scaffidi, M. T. Waters, S. M. Smith, Stereospecificity in strigolactone biosynthesis and perception. *Planta* **243**, 1361–1373 (2016).
26. H. M. Ghebrehiwot *et al.*, Karrikinolide residues in grassland soils following fire: Implications on germination activity. *S. Afr. J. Bot.* **88**, 419–424 (2013).
27. J. Kochanek, R. L. Long, A. T. Lisle, G. R. Flematti, Karrikins identified in biochars indicate post-fire chemical cues can influence community diversity and plant development. *PLoS One* **11**, e0161234 (2016).
28. C. E. Conn, D. C. Nelson, Evidence that KARRIKIN-INSENSITIVE2 (KAI2) receptors may perceive an unknown signal that is not karrikin or strigolactone. *Front Plant Sci* **6**, 1219 (2016).
29. M. T. Waters *et al.*, A Selaginella moellendorffii Ortholog of KARRIKIN INSENSITIVE2 functions in Arabidopsis development but cannot mediate responses to karrikins or strigolactones. *Plant Cell* **27**, 1925–1944 (2015).
30. Y. K. Sun, G. R. Flematti, S. M. Smith, M. T. Waters, Reporter gene-facilitated detection of compounds in Arabidopsis leaf extracts that activate the karrikin signaling pathway. *Front Plant Sci* **7**, 1799 (2016).
31. J. Yao *et al.*, Desmethyl butenolides are optimal ligands for karrikin receptor proteins. *New Phytol.* **230**, 1003–1016 (2021).
32. C. Gutjahr *et al.*, Rice perception of symbiotic arbuscular mycorrhizal fungi requires the karrikin receptor complex. *Science* **350**, 1521–1524 (2015).
33. J. Choi *et al.*, The negative regulator SMAX1 controls mycorrhizal symbiosis and strigolactone biosynthesis in rice. *Nat. Commun.* **11**, 2114 (2020).
34. I. Soundappan *et al.*, SMAX1-LIKE/D53 family members enable distinct MAX2-dependent responses to strigolactones and karrikins in Arabidopsis. *Plant Cell* **27**, 3143–3159 (2015).
35. W. Li *et al.*, The karrikin receptor KAI2 promotes drought resistance in Arabidopsis thaliana. *PLoS Genet.* **13**, e1007076 (2017).
36. L. Wang, M. T. Waters, S. M. Smith, Karrikin-KAI2 signalling provides Arabidopsis seeds with tolerance to abiotic stress and inhibits germination under conditions unfavourable to seedling establishment. *New Phytol.* **219**, 605–618 (2018).
37. J. A. Villaécija-Aguilar *et al.*, SMAX1/SMXL2 regulate root and root hair development downstream of KAI2-mediated signalling in Arabidopsis. *PLoS Genet.* **15**, e1008327 (2019).
38. Y. Mizuno *et al.*, Major components of the KARRIKIN INSENSITIVE2-dependent signaling pathway are conserved in the liverwort Marchantia polymorpha. *Plant Cell* **33**, 2395–2411 (2021).
39. Y. Guo, Z. Zheng, J. J. La Clair, J. Chory, J. P. Noel, Smoke-derived karrikin perception by the α/β -hydrolase KAI2 from Arabidopsis. *Proc. Natl. Acad. Sci. U.S.A.* **110**, 8284–8289 (2013).
40. M. Kagiya *et al.*, Structures of D14 and D14L in the strigolactone and karrikin signaling pathways. *Genes Cells* **18**, 147–160 (2013).
41. S. Toh, D. Holbrook-Smith, M. E. Stokes, Y. Tsuchiya, P. McCourt, Detection of parasitic plant suicide germination compounds using a high-throughput Arabidopsis HTL/KAI2 strigolactone perception system. *Chem. Biol.* **21**, 988–998 (2014).
42. Y. Xu *et al.*, Structural basis of unique ligand specificity of KAI2-like protein from parasitic weed *Striga hermonthica*. *Sci. Rep.* **6**, 31386 (2016).
43. Y. Xu *et al.*, Structural analysis of HTL and D14 proteins reveals the basis for ligand selectivity in *Striga*. *Nat. Commun.* **9**, 3947 (2018).
44. I. Lee *et al.*, A missense allele of KARRIKIN-INSENSITIVE2 impairs ligand-binding and downstream signaling in Arabidopsis thaliana. *J. Exp. Bot.* **69**, 3609–3623 (2018).
45. M. Bürger *et al.*, Structural basis of karrikin and non-natural strigolactone perception in *Physcomitrella patens*. *Cell Rep.* **26**, 855–865.e5 (2019).
46. C. Hamiaux *et al.*, DAD2 is an α/β hydrolase likely to be involved in the perception of the plant branching hormone, strigolactone. *Curr. Biol.* **22**, 2032–2036 (2012).
47. R. Yao *et al.*, ShHTL7 is a non-canonical receptor for strigolactones in root parasitic weeds. *Cell Res.* **27**, 838–841 (2017).
48. C. Hamiaux *et al.*, Inhibition of strigolactone receptors by *N*-phenylanthranilic acid derivatives: Structural and functional insights. *J. Biol. Chem.* **293**, 6530–6543 (2018).
49. C. E. Conn *et al.*, PLANT EVOLUTION. Convergent evolution of strigolactone perception enabled host detection in parasitic plants. *Science* **349**, 540–543 (2015).
50. R. Bythell-Douglas *et al.*, Evolution of strigolactone receptors by gradual neo-functionalization of KAI2 paralogues. *BMC Biol.* **15**, 52 (2017).
51. C. V. Ha *et al.*, Positive regulatory role of strigolactone in plant responses to drought and salt stress. *Proc. Natl. Acad. Sci. U.S.A.* **111**, 851–856 (2014).
52. K. Bursch, E. T. Niemann, D. C. Nelson, H. Johansson, Karrikins control seedling photomorphogenesis and anthocyanin biosynthesis through a HYS-BBX transcriptional module. *Plant J.* **107**, 1346–1362 (2021).
53. K. Mashiguchi *et al.*, Feedback-regulation of strigolactone biosynthetic genes and strigolactone-regulated genes in Arabidopsis. *Biosci. Biotechnol. Biochem.* **73**, 2460–2465 (2009).
54. E. P. Risseuw *et al.*, Protein interaction analysis of SCF ubiquitin E3 ligase subunits from Arabidopsis. *Plant J.* **34**, 753–767 (2003).
55. Arabidopsis Interactome Mapping Consortium, Evidence for network evolution in an Arabidopsis interactome map. *Science* **333**, 601–607 (2011).
56. J. Jumper *et al.*, Highly accurate protein structure prediction with AlphaFold. *Nature* **596**, 583–589 (2021).
57. Z.-P. Wang *et al.*, Egg cell-specific promoter-controlled CRISPR/Cas9 efficiently generates homozygous mutants for multiple target genes in Arabidopsis in a single generation. *Genome Biol.* **16**, 144 (2015).
58. A. Khosla, C. Rodriguez-Furlan, S. Kapoor, J. M. Van Norman, D. C. Nelson, A series of dual-reporter vectors for ratiometric analysis of protein abundance in plants. *Plant Direct* **4**, e00231 (2020).
59. M. T. Waters, A. Scaffidi, G. Flematti, S. M. Smith, Substrate-induced degradation of the α/β -fold hydrolase KARRIKIN INSENSITIVE2 requires a functional catalytic triad but is independent of MAX2. *Mol. Plant* **8**, 814–817 (2015).
60. M. T. Waters, S. M. Smith, KAI2- and MAX2-mediated responses to karrikins and strigolactones are largely independent of HYS in Arabidopsis seedlings. *Mol. Plant* **6**, 63–75 (2013).
61. A. R. F. White, J. A. Mendez, A. Khosla, D. C. Nelson, Rapid analysis of strigolactone receptor activity in a *Nicotiana benthamiana* dwarf14 mutant. *Plant Direct*, in press.
62. N. Schumann, A. Navarro-Quezada, K. Ullrich, M. Quint, Molecular evolution and selection patterns of plant F-box proteins with C-terminal kelch repeats. *Plant Physiol.* **155**, 835–850 (2011).
63. M. Lopez-Obando *et al.*, *Physcomitrella patens* MAX2 characterization suggests an ancient role for this F-box protein in photomorphogenesis rather than strigolactone signalling. *New Phytol.* **219**, 743–756 (2018).
64. J. Zheng *et al.*, Karrikin signaling acts parallel to and additively with strigolactone signaling to regulate rice mesocotyl elongation in darkness. *Plant Cell* **32**, 2780–2805 (2020).
65. S. C. Kerr *et al.*, Hormonal regulation of the BRC1-dependent strigolactone transcriptome involved in shoot branching responses. *bioRxiv* [Preprint] (2020). <https://doi.org/10.1101/2020.03.19.999581> (Accessed 25 March 2020).
66. S. Carbonnel *et al.*, Lotus japonicus karrikin receptors display divergent ligand-binding specificities and organ-dependent redundancy. *PLoS Genet.* **16**, e1009249 (2020).
67. M. Hamon-Josse *et al.*, KAI2 regulates seedling development by mediating light-induced remodelling of auxin transport. *bioRxiv* [Preprint] (2021). <https://doi.org/10.1101/2021.05.06.443001> (Accessed 13 May 2021).
68. P. Stirnberg, K. van De Sande, H. M. O. Leyser, MAX1 and MAX2 control shoot lateral branching in Arabidopsis. *Development* **129**, 1131–1141 (2002).
69. K. Xie, J. Zhang, Y. Yang, Genome-wide prediction of highly specific guide RNA spacers for CRISPR-Cas9-mediated genome editing in model plants and major crops. *Mol. Plant* **7**, 923–926 (2014).
70. H.-L. Xing *et al.*, A CRISPR/Cas9 toolkit for multiplex genome editing in plants. *BMC Plant Biol.* **14**, 327 (2014).
71. T. Nakagawa *et al.*, Improved gateway binary vectors: High-performance vectors for creation of fusion constructs in transgenic analysis of plants. *Biosci. Biotechnol. Biochem.* **71**, 2095–2100 (2007).